THE BELL SYSTEM TECHNICAL JOURNAL
Vol. 55, No. 4, April 1976
Printed in U.S.A.

Spectral Occupancy of Digital Angle-Modulation Signals

By V. K. PRABHU

(Manuscript received December 2, 1975)

The spectral or band occupancy of an RF signal is often defined as the bandwidth that contains a specified fraction (usually 99 percent) of the modulated RF power. The band occupancy of binary and quaternary PSK signals with and without RF filtering and with modulation pulses of several shapes has been evaluated and the results presented in graphical and tabular form. For a binary FSK signal with phase deviation of $\pm\pi/2$, sometimes called an FM-PSK signal, numerical values of the spectral occupancy with rectangular and raised-cosine signaling have been obtained and the results given in graphical form. For a binary PSK signal with signaling rate $1/T$ and with arbitrary baseband pulse shaping, we have derived a lower bound on the fraction of the continuous power contained outside any given band, but have not been able to get a bound on the total band occupancy. However, for an FM-PSK signal, a lower bound on the total band occupancy has been derived, and it is shown that the value of this lower bound for 99-percent power occupancy is $1.117/T$. The 99-percent power occupancy bandwidth of an FM-PSK signal is $1.170/T$ with rectangular signaling and $2.20/T$ with raised-cosine signaling.

I. INTRODUCTION AND SUMMARY

Efficiency of use of the radio spectrum has recently become the subject of increased attention since terrestrial and satellite communication needs have placed an increasing burden on the available RF bands.[1,2] For spectrum conservation, the band occupancy of the chosen modulation scheme must be small so that as many channels as possible can be accommodated in a given band. Since the band occupancy of analog signals has been extensively discussed in the literature,[3–5] we shall deal here only with digital signals.

For radio systems, the "occupied bandwidth" is often specified by the spectral band which contains a certain fraction of the total RF power.* The Federal Communications Commission (FCC) presently

* For analog FM systems, an alternate way of specifying bandwidth is discussed in Ref. 5.

specifies this power to be 99 percent and requires that not more than 1 percent of the power be contained outside the assigned band.[6] For radio transmission using digital modulation techniques, the additional requirements presently specified by the FCC are in terms of the spectral density of out-of-band emission rather than just total out-of-band power.* For operating frequencies below (above) 15 GHz, the attenuation A, expressed in dB and equal to the mean output power divided by the power measured in any 4-kHz (1-MHz) band, the center frequency of which differs from the assigned frequency by 50 percent or more of the authorized bandwidth, shall not be less than 50 dB (11 dB) and shall satisfy the relation $A \geqq 35 + 0.8\ (P - 50) + 10 \log_{10} B$ for operating frequencies below 15 GHz and the relation $A \geqq 11 + 0.4\ (P - 50) + 10 \log_{10} B$ for operating frequencies above 15 GHz where P is the percent difference from the carrier frequency and B is the authorized bandwidth in megahertz. For operating frequencies below (above) 15 GHz, attenuation greater than 80 dB (56 dB) is not required for any value of P. While this is the "necessary bandwidth" specified by the FCC, the quantity "occupied bandwidth" still remains as one of the parameters used to specify the assigned band.†

The spectral occupancy of binary and quaternary PSK signals with nonoverlapping pulses of several shapes has been determined and the results presented in graphical form. The 99-percent power occupancy band of a PSK signal with rectangular signaling is extremely large; hence, for this case we also give the band occupancy when different RF filters are used to confine the spectrum.

By using the classical work of Slepian, Landau, and Pollak,[8,9] we derive a lower bound on the fractional power, contained outside any given band, of the *continuous part* of the binary PSK spectrum.[10] It is shown that the lower bound can be achieved if the baseband pulse is the inverse sine function of a certain prolate spheroidal wave function. It is also shown that the smaller the value of the lower bound, the smaller the amount of total power that can be contained in the continuous part (the total RF power has been normalized to unity). We have not been able to get a bound on the total fractional power that may be contained outside the assigned band of a binary PSK signal or find an optimum pulse shape if the total power contained in the continuous part is assumed to be a specified fraction of the total RF power.

For a binary PSK signal with phase deviation of $\pm\pi/2$, sometimes called an FM-PSK signal, numerical values of the spectral occupancy

* For details, see FCC Docket 19311, FCC 71-940, adopted September 8, 1971, released September 15, 1971; FCC 73-445, adopted May 3, 1973, released May 8, 1973; FCC 74-985, adopted September 19, 1974, released September 27, 1974.

† Another method of determining "sufficient bandwidth" for PSK systems is discussed in Ref. 7.

with rectangular and raised-cosine signaling have been obtained and the results are given in graphical form. For such a binary FSK signal with arbitrary baseband pulse shaping, a lower bound on the *total* band occupancy has been derived, and it is shown that the value of this lower bound for 99-percent power occupancy is $1.117/T$, where T is the signal interval. The 99-percent power occupancy bandwidth of an FM-PSK signal is $1.170/T$ with rectangular signaling and $2.20/T$ with raised-cosine signaling. The good spectral properties of an FM-PSK signal with rectangular signaling are well known,[11] and it may be detected as a PSK signal with the same bit error rate performance as that of BPSK.[12]

II. SPECTRAL OCCUPANCY OF DIGITAL SIGNALS

In our analysis for PSK and FM-PSK systems, we assume that the baseband signaling pulses have a common shape and that all signaling pulses are equally likely. We also assume that symbols transmitted during different time slots are statistically independent and identically distributed.

If the digital angle-modulated (PSK or FSK) wave is represented as

$$x(t) = \mathrm{Re} \exp \{j[2\pi f_c t + \Phi(t) + \theta]\}, \tag{1}$$

it is shown in Refs. 10 and 13 that the power spectral density $\mathbf{P}_x(f)$ of $x(t)$ can be expressed as

$$\mathbf{P}_x(f) = \tfrac{1}{4}\mathbf{P}_v(f - f_c) + \tfrac{1}{4}\mathbf{P}_v(-f - f_c), \tag{2}$$

where $\mathbf{P}_v(f)$ is the power spectral density of

$$v(t) = e^{j\Phi(t)} \tag{3}$$

and f_c is the carrier frequency. In (1), θ is assumed to be a random variable uniformly distributed over $[0, 2\pi)$.

The fractional power Δ^2 contained outside the band $[f_c - W, f_c + W]$ can be shown to be

$$\Delta^2 = 2 \int_W^\infty \mathbf{P}_v(f)df - \int_{2f_c-W}^{2f_c+W} \mathbf{P}_v(f)df. \tag{4}$$

In most cases of practical interest, $\mathbf{P}_v(f)$ is a rapidly decreasing function of f, $f_c/W \gg 1$, and*

$$\Delta^2 = 2 \int_W^\infty \mathbf{P}_v(f)df. \tag{5}$$

* Since $\mathbf{P}_v(f) \geqq 0$, $\Delta^2 \leqq 2 \int_W^\infty \mathbf{P}_v(f)df$ for any f_c/W.

2.1 Spectral density of an M-ary PSK signal

For an M-ary PSK signal (we assume $M = 2^N$, N an integer) with signaling rate $1/T$,

$$\Phi(t) = \sum_{k=-\infty}^{\infty} \underline{\mathbf{a}_k} \cdot g(t - kT)], \tag{6}$$

where $\mathbf{a}_k$ is a vector-valued stationary random process and $\mathbf{g}(t)]$ are the pulse shapes corresponding to the M symbols.

If the signaling pulses in different time slots never overlap, it is shown in Ref. 10 that $\mathbf{P}_v(f)$ consists of a line component part $\mathbf{P}_{vl}(f)$ and a continuous part $\mathbf{P}_{vc}(f)$, $\mathbf{P}_v(f) = \mathbf{P}_{vl} + \mathbf{P}_{vc}(f)$,

$$\mathbf{P}_{vl}(f) = \frac{1}{T^2} |\underline{\mathbf{w}} \cdot \mathbf{R}(f)]| \sum_{n=-\infty}^{\infty} \delta\left(f - \frac{n}{T}\right), \tag{7}$$

$$\mathbf{P}_{vc}(f) = \frac{1}{2T} \sum_{i=1}^{M} \sum_{j=1}^{M} w_i w_j |R_i(f) - R_j(f)|^2, \tag{8}$$

where $\underline{\mathbf{w}} = [w_1, w_2, \cdots, w_M]$, w_i is the probability that the ith signaling waveform $g_i(t)$ is transmitted in any time slot and $R_i(f)$ is the Fourier transform of $r_i(t)$,

$$r_i(t) = \begin{cases} \exp[jg_i(t)], & 0 < t \leqq T \\ 0 \quad , & \text{otherwise.} \end{cases} \tag{9}$$

Since we assume that the M signaling pulses have a common shape,

$$\underline{\mathbf{g}(t)} = [\alpha_1, \alpha_2, \cdots, \alpha_M] g(t), \tag{10}$$

where α_i is the peak phase value of the ith symbol and the maximum value of $g(t)$ has been normalized to unity.

From (5),

$$\Delta^2 = \Delta_l^2 + \Delta_c^2, \tag{11}$$

where

$$\Delta_l^2 = 2 \int_W^{\infty} \mathbf{P}_{vl}(\mu) d\mu = \text{the fractional part of line power contained outside the band} \tag{12}$$

and

$$\Delta_c^2 = 2 \int_W^{\infty} \mathbf{P}_{vc}(\mu) d\mu = \text{the fractional part of continuous power contained outside the band.} \tag{13}$$

2.2 Spectral density of an M-ary FSK signal

For an M-ary FSK signal,[13]

$$\Phi(t) = \int^t f_d(\mu) d\mu, \tag{14}$$

$$f_d(t) = \sum_{k=-\infty}^{\infty} \underline{\mathbf{a}_k} \cdot \mathbf{h}(t - kT)], \qquad \underline{\mathbf{h}(t)} = \underline{0},\ t \leqq 0,\ t > T, \tag{15}$$

$$\mathbf{P}_v(f) = \frac{1}{T} \underline{\mathbf{R}(f)} \cdot (\mathbf{A} + \mathbf{A}^\dagger) \cdot \mathbf{R}^*(f)], \tag{16}$$

where

$$\mathbf{A} = \frac{1}{2}\mathbf{w}_d + \frac{e^{-j2\pi fT}\mathbf{w}] \cdot \underline{\mathbf{r}(T)} \cdot \mathbf{w}_d}{1 - e^{-j2\pi fT}\underline{\mathbf{w}} \cdot \mathbf{r}(T)]}, \qquad |\underline{\mathbf{w}} \cdot \mathbf{r}(T)]| < 1, \tag{17}$$

$$\mathbf{w}_d = \begin{bmatrix} w_1 & & & & 0 \\ & w_2 & & & \\ & & \cdot & & \\ & & & \cdot & \\ & & & & \cdot \\ 0 & & & & w_M \end{bmatrix}, \tag{18}$$

$R_i(f)$ is the Fourier transform of $r_i(t)$, and

$$r_i(t) = \begin{cases} \exp\left[j \int_0^t h_i(\mu) d\mu\right], & 0 < t \leqq T \\ 0 \quad , & \text{otherwise.} \end{cases} \tag{19}$$

We make the same assumptions for FSK as for PSK. However, note that $\mathbf{P}_v(f)$ does not contain any lines if $\mathbf{w}]$ and $\mathbf{r}(t)]$ satisfy the inequality in (17). Since spectral lines do not often contain any useful information (except for carrier recovery), their presence indicates nonoptimum pulse shaping. In this paper, we shall not consider FSK with spectral lines. For FSK, $\Delta^2 = \Delta_c^2$ from (5).

III. BAND OCCUPANCY OF A BINARY PSK SIGNAL

For binary PSK, we assume that $\alpha_1 = -\alpha_2 = \pi/2$ and that both symbols are equally likely. From (8),

$$\mathbf{P}_{v_c}(f) = \frac{1}{4T} |R_1(f) - R_2(f)|^2, \tag{20}$$

where

$$\begin{aligned} R_1(f) - R_2(f) &= \int_0^T [e^{j(\pi/2)g(t)} - e^{-j(\pi/2)g(t)}]e^{-j2\pi ft}dt \\ &= 2j \int_0^T \sin\left\{\frac{\pi}{2} g(t)\right\} e^{-j2\pi ft}dt. \end{aligned} \tag{21}$$

For rectangular, cosinusoidal, raised-cosinusoidal, trapezoidal, and triangular $g(t)$, we have calculated $\mathbf{P}_v(f)$ from (7) and (8) and Δ^2 from (5). For these cases, the total out-of-band power ratio Δ^2 for binary PSK is plotted in Figs. 1 and 2. The 99-percent (or any other fractional) power bandwidth occupancy for binary PSK may be determined from

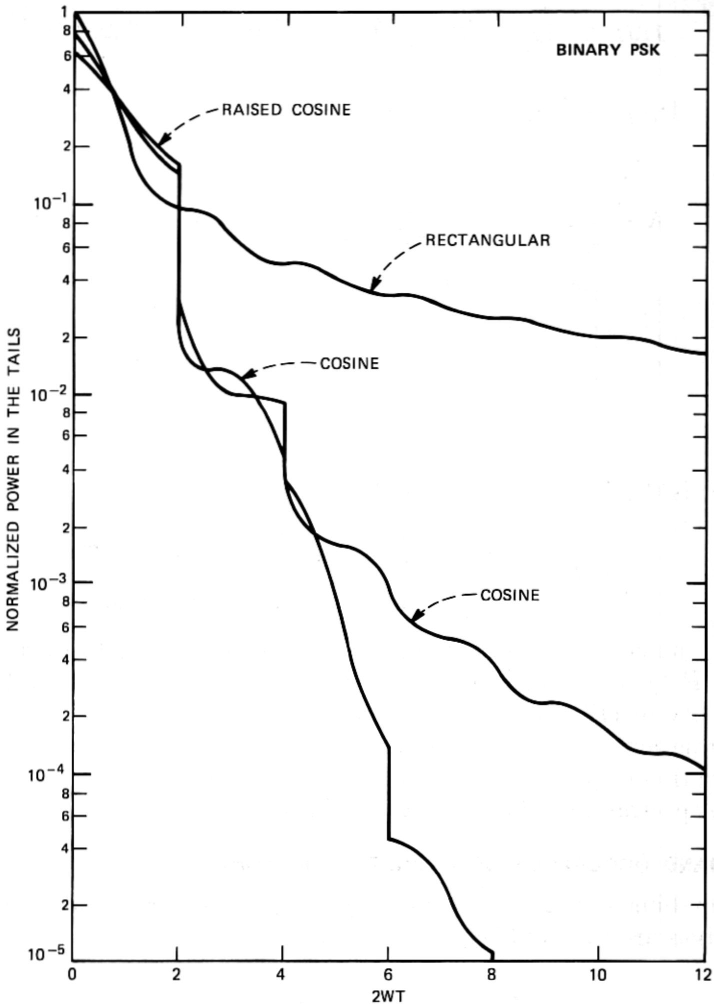

Fig. 1—Normalized power contained outside the band $[-W, W]$ for binary PSK with different baseband signaling waveforms.

these figures. Since the 99-percent power occupancy of binary PSK with rectangular signaling is very large, we show the bandwidth occupancy with RF filtering in Figs. 3, 4, and 5.

IV. BAND OCCUPANCY OF A QPSK SIGNAL

For QPSK modulation and for equally likely symbols,

$$\mathbf{P}_{v_c}(f) = \frac{1}{32T} \sum_{i=1}^{4} \sum_{j=1}^{4} |R_i(f) - R_j(f)|^2, \tag{22}$$

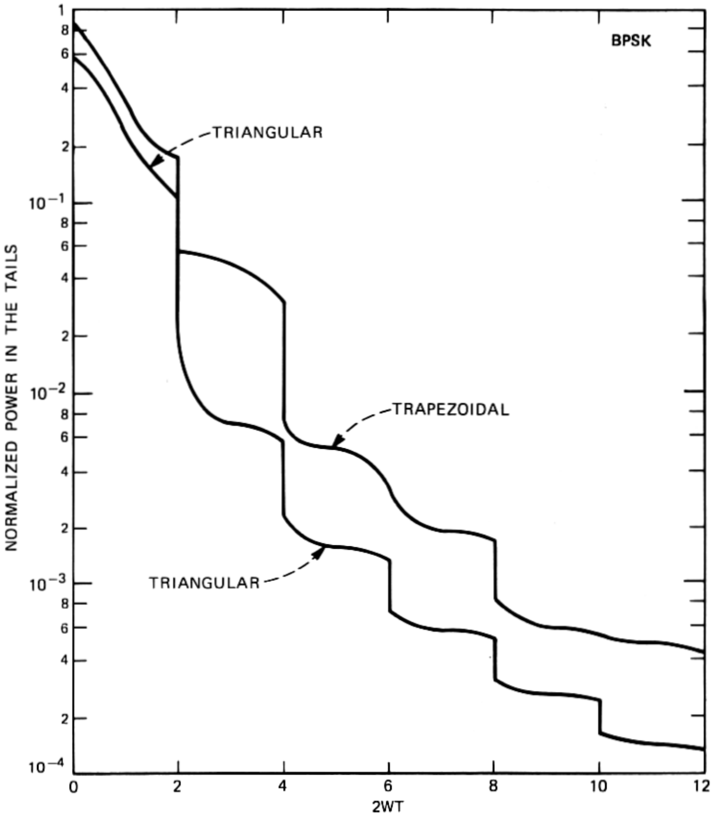

Fig. 2—Normalized power contained outside the band $[-W, W]$ for binary PSK with different baseband signaling waveforms.

where $R_l(f)$ is the Fourier transform of $r_l(t)$,

$$r_l(t) = \begin{cases} \exp[j\alpha_l g(t)], & 0 < t \leqq T \\ 0 \quad , & \text{otherwise,} \end{cases} \tag{23}$$

and

$$\alpha_l = (2l - 5)\frac{\pi}{4}, \qquad l = 1, 2, 3, 4. \tag{24}$$

$\mathbf{P}_{vl}(f)$ is given by (7).

For rectangular, cosinusoidal, raised-cosinusoidal, trapezoidal, and triangular $g(t)$, we have calculated $\mathbf{P}_v(f)$ from (7) and (8) and Δ^2 from (5). For these cases, the total out-of-band power ratio Δ^2 is plotted in Figs. 6 and 7. The 99-percent (or any other fractional) power bandwidth occupancy for quaternary PSK may be determined from these figures. Since the spectral density of QPSK with rectangular signaling

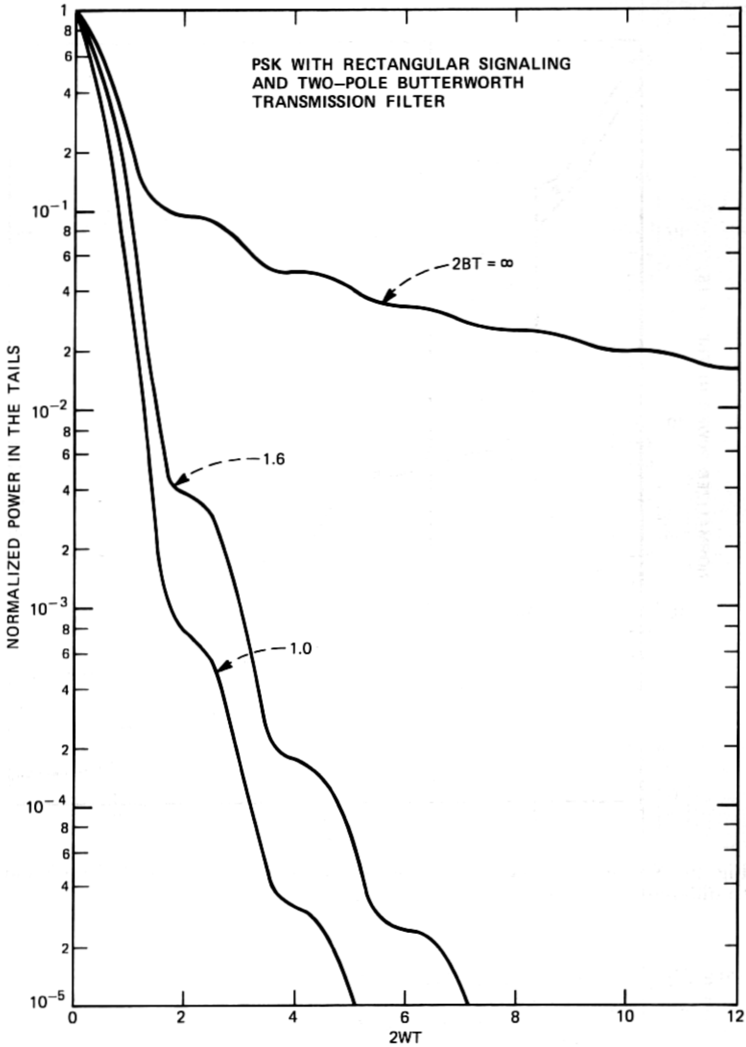

Fig. 3—Normalized power contained outside the band $[-W, W]$ for M-ary PSK ($M = 2^N$, $N \geqq 1$) with rectangular signaling and a two-pole Butterworth transmission filter. The squared amplitude characteristic of the equivalent low-pass filter is assumed to be given by $|H_T(f)|^2 = 1/[1 + (f/A)^4]$, where $2B = 2A(\pi/4)/\sin \pi/4$ is the noise bandwidth of the filter.

is the same as that of BPSK, the bandwidth occupancy of QPSK with RF filtering is also given by Figs. 3, 4, and 5.

V. BAND OCCUPANCY OF AN FM-PSK SIGNAL

A binary FM-PSK signal is a special case of the binary continuous-phase FSK modulation where the phase deviation in one signaling

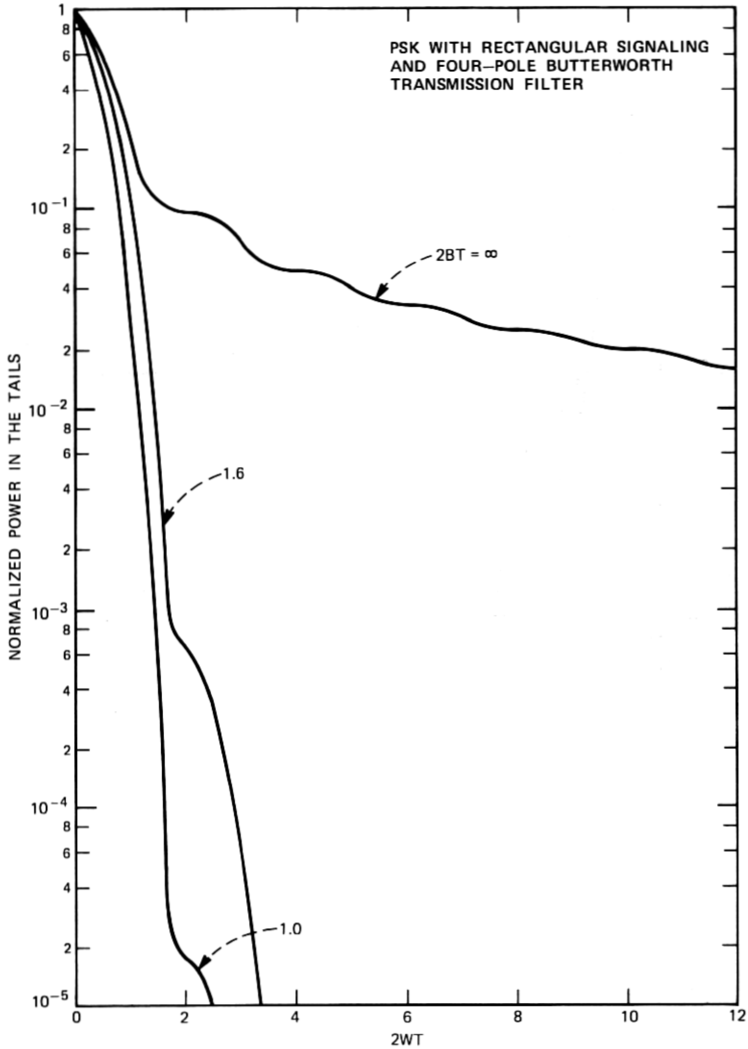

Fig. 4—Normalized power contained outside the band $[-W, W]$ for M-ary PSK ($M = 2^N$, $N \geqq 1$) with rectangular signaling and a four-pole Butterworth transmission filter. The squared amplitude characteristic of the equivalent low-pass filter is assumed to be given by $|H_T(f)|^2 = 1/[1 + (f/A)^8]$, where $2B = 2A(\pi/8)/\sin \pi/8$ is the noise bandwidth of the filter.

interval is $\pm\pi/2$ and which can be detected as a PSK signal. Note that one may use a four-phase demodulator to detect a binary FM-PSK signal* to have the same bit error rate performance as that of BPSK.[14–16]

* A form of binary FM-PSK can be shown to be equal to the sum of two offset quadrature-phase binary PSK signals. A form of it is, therefore, sometimes referred to as offset QPSK (Ref. 2). An FM-PSK with rectangular frequency modulation signaling is called fast FSK in Ref. 12 and MSK in Ref. 14.

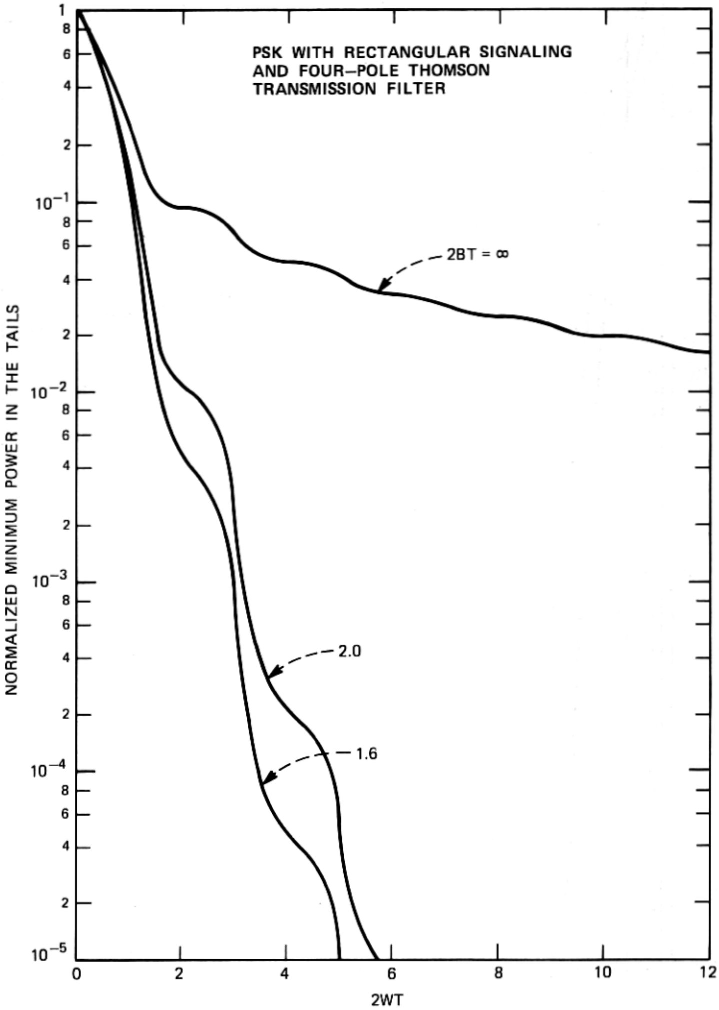

Fig. 5—Normalized power contained outside the band $[-W, W]$ for M-ary PSK ($M = 2^N$, $N \geqq 1$) with rectangular signaling and a four-pole Thomson transmission filter. The squared amplitude characteristic of the equivalent low-pass filter is assumed to be given by $|H_T(f)|^2 = 11025/(z^8 + 10z^6 + 135z^4 + 1575z^2 + 11025)$, $z = f/A$ and $2B = 4.4238A$ is the noise bandwidth of the filter.

There are no discrete lines in the FM-PSK spectrum, but standard techniques (such as the Costas loop) can be used to recover the coherent carrier (it is necessary to use differential encoding or prior knowledge of framing polarity, etc., to resolve the ambiguity present in the phase of the recovered carrier).[12]

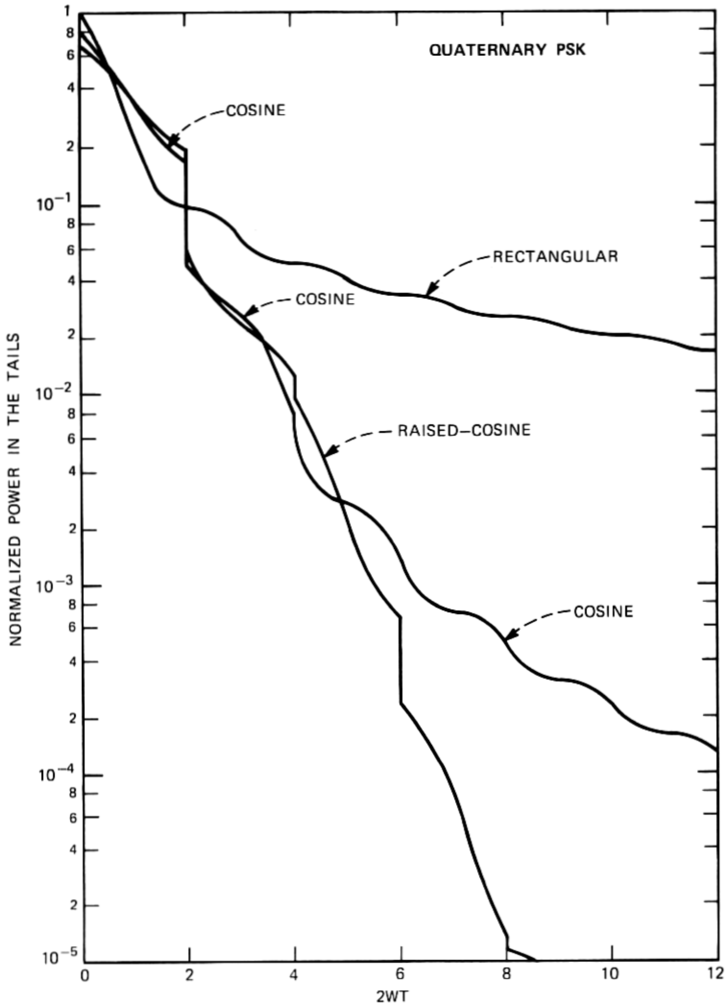

Fig. 6—Normalized power contained outside the band $[-W, W]$ for quaternary PSK with different baseband signaling waveforms.

To get the spectral density of binary FSK, we put

$$r(T)] = \begin{matrix} e^{j(\pi/2)} \\ e^{-j(\pi/2)} \end{matrix} \Bigg] \tag{25}$$

in (16), (17), and (19) for any baseband signaling waveform $h(t)$. We assume that we transmit $+1$ by shifting the carrier frequency by $+f_d g(t)$, $0 < t \leqq T$, and -1 by shifting the carrier frequency by

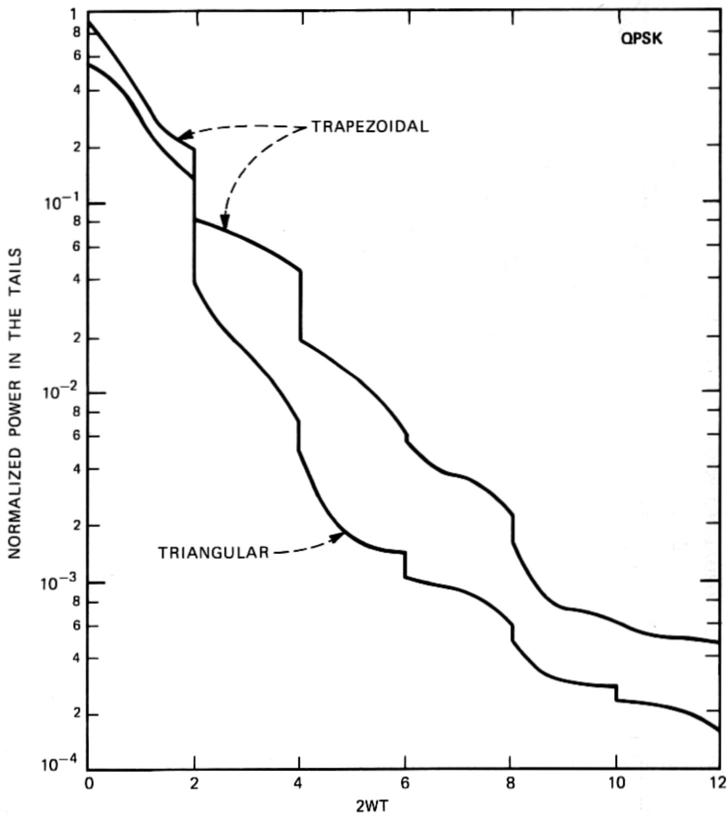

Fig. 7—Normalized power contained outside the band $[-W, W]$ for quaternary PSK with different baseband signaling waveforms.

$-f_d g(t)$, $0 < t \leqq T$. For rectangular signaling,

$$f_d = \frac{1}{4}\frac{1}{T}, \tag{26}$$

and for raised-cosine signaling,

$$f_d = \frac{1}{2}\frac{1}{T}, \tag{27}$$

so that the peak frequency deviation with raised-cosine signaling is larger than that with rectangular signaling.

From (16), (17), and (25) one can show that the spectral density $\mathbf{P}_v(f)$ of binary FM-PSK is

$$\mathbf{P}_v(f) = \mathbf{P}_{v_e}(f) = \frac{1}{T} \underline{R_1 \, R_2} \cdot \begin{bmatrix} \frac{1}{2}\{1 + \sin(2\pi f T)\} & -\frac{j}{2}\cos(2\pi f T) \\ \frac{j}{2}\cos(2\pi f T) & \frac{1}{2}\{1 - \sin(2\pi f T)\} \end{bmatrix} \cdot \begin{bmatrix} R_1^* \\ R_2^* \end{bmatrix}, \quad (28)$$

where R_1, R_2 are the Fourier transforms of $r_1(t)$, $r_2(t)$

$$r_1(t) = \begin{cases} \exp\left[j2\pi f_d \int_0^t g(t)dt\right], & 0 < t \leqq T \\ 0 \qquad , & \text{otherwise,} \end{cases} \quad (29)$$

$$r_2(t) = \begin{cases} \exp\left[-j2\pi f_d \int_0^t g(t)dt\right], & 0 < t \leqq T \\ 0 \qquad , & \text{otherwise.} \end{cases} \quad (30)$$

For rectangular and raised-cosine signaling, we plot for binary FM-PSK the out-of-band power ratio Δ^2 in Fig. 8. The 99-percent (or any other fractional) power bandwidth occupancy may be determined from results given in this figure.

VI. TIME-LIMITED AND BAND-LIMITED SIGNALS

We shall derive the lower bound on the band occupancy of binary PSK and FSK signals by using the results obtained for time-limited and band-limited functions.

In their classical papers, Slepian, Landau, and Pollak have derived[8,9] the pulse waveform of given duration that has a maximum of its energy concentrated below a certain frequency band. These optimum pulse waveforms are the well-known prolate spheroidal wave functions. A widespread opinion is that pulses with minimum energy at high frequencies should have a rounded form with many continuous derivatives. Since the optimum pulses (the prolate spheroidal wave functions) are usually not continuous at the limits of their truncation interval, this opinion does not seem to be justified. In fact, Hilberg and Rothe[17] have shown recently that constraints of continuous derivatives tend to increase the total out-of-band energy. We shall now state the bounds given by Slepian, Landau, and Pollak.

If we define

$$\alpha^2 = \frac{\int_{t_0 - T'/2}^{t_0 + T'/2} |f(t)|^2 dt}{\int_{-\infty}^{\infty} |f(t)|^2 dt}, \quad (31)$$

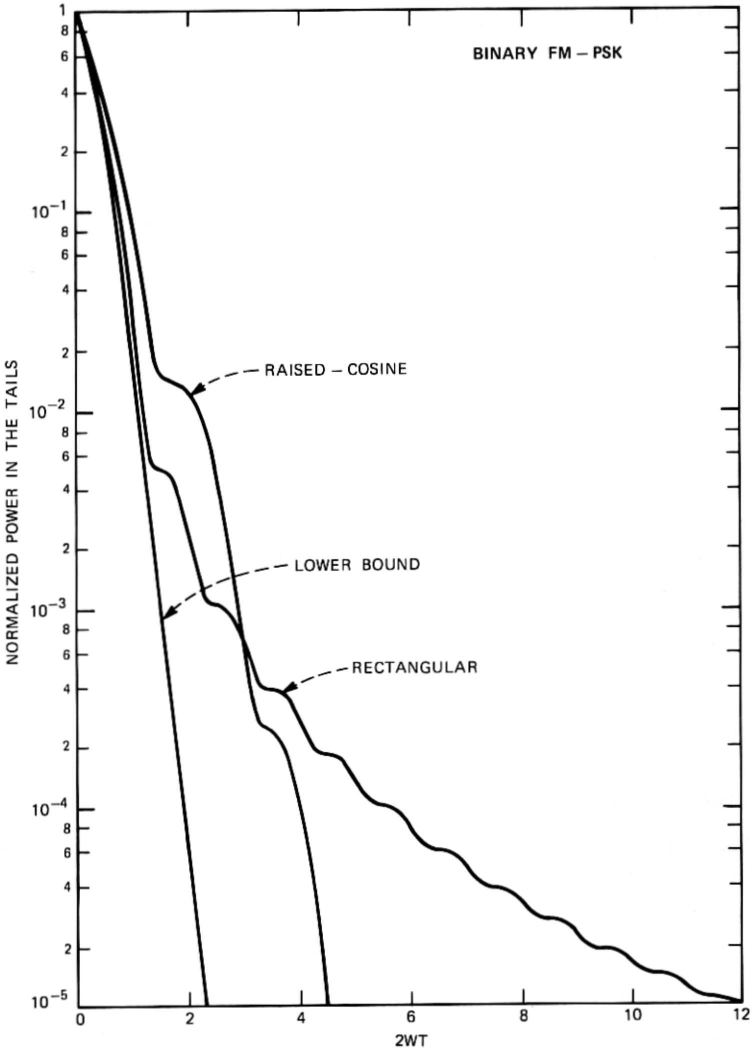

Fig. 8—Normalized power Δ^2 contained outside the band $[-W, W]$ for binary FM-PSK with different baseband signaling waveforms and also the lower bound on Δ^2 for any baseband signaling waveform.

and

$$\beta^2 = \frac{\int_{-W}^{W} |F(f)|^2 df}{\int_{-\infty}^{\infty} |F(f)|^2 df}, \qquad F(f) = \int_{-\infty}^{\infty} f(t) e^{-j2\pi f t} dt, \tag{32}$$

it is shown in Ref. 9 that

$$\cos^{-1}(\alpha) + \cos^{-1}(\beta) \geqq \cos^{-1}\sqrt{\lambda_0}, \tag{33}$$

where λ_0 is the largest eigenvalue of the integral equation

$$\lambda f(t) = \frac{1}{\pi} \int_{-(T'/2)}^{T'/2} f(s) \frac{\sin\{2\pi W(t-s)\}}{(t-s)} ds. \tag{34}$$

In (31), we assume that $f(t) \in \mathcal{L}^2_\infty$ where $\mathcal{L}^2_\infty$ is the set of all complex-valued functions defined on the real line and integrable in absolute square [$f(t)$ has finite energy].

In binary PSK and certain binary FSK, we shall show that $\mathbf{P}_v(f)$ or $\mathbf{P}_{vc}(f)$ can be expressed as the energy density spectrum [$|X(f)|^2$] of a certain $x(t)$, time-limited to a duration T_{eq}.* From (31), if $x(t)$ is of duration T_{eq},

$$\begin{gathered} \alpha^2 = 1, \qquad T' = T_{eq}, \\ \beta^2 \leqq \lambda_0 \end{gathered} \tag{35}$$

and the maximum value of β^2 is attained when $x(t)$ is a prolate spheroidal wave function $\psi_0(t, d)$ given in Refs. 8 and 9, $d = \pi W T_{eq}$. The fractional energy Λ^2 contained outside the band $[-W, W]$ is, therefore, lower-bounded by

$$\Lambda^2 = 1 - \beta^2 \geqq 1 - \lambda_0 = \Lambda^2_{min}. \tag{36}$$

The values of Λ^2_{min} computed from the relations given in Refs. 8, 9, and 18 are shown in Fig. 9. It therefore follows that it is impossible to find an $\mathcal{L}^2$-integrable pulse waveform $x(t)$ which has a duration T_{eq} and which has a fractional energy less than $\Lambda^2_{min}(WT_{eq})$ outside the band $[-W, W]$.

VII. LOWER BOUND ON THE BAND OCCUPANCY OF PSK AND FM-PSK SIGNALS

Let us first consider the band occupancy of the continuous part $\mathbf{P}_{vc}(f)$ of a BPSK spectrum.

From (20) and (21),

$$\mathbf{P}_{vc}(f) = |X(f)|^2, \tag{37}$$

where $X(f)$ is the Fourier transform of

$$x(t) = \begin{cases} \dfrac{\sin\left\{\dfrac{\pi}{2} g(t)\right\}}{\sqrt{T}}, & 0 < t \leqq T \\ 0 \quad , & \text{otherwise.} \end{cases} \tag{38}$$

In (37) we have expressed the continuous part of the spectral density of a binary PSK signal in terms of the energy density spectrum

* In FM-PSK, it will turn out that $T_{eq} = 2T$, where T is the duration of the signaling waveform $g(t)$. Hence, we use the symbol T_{eq} to denote the duration of $x(t)$.

of an arbitrary pulse waveform $x(t) \in \Omega \subset \mathcal{L}^2_\infty$.* $x(t)$ can be nonzero only for $0 < t \leqq T$. From Section VI, it therefore follows that the out-of-band power ratio Λ_c^2 of a binary PSK signal is lower-bounded by

$$\Lambda_c^2 \geqq \Lambda_{\min}^2(WT), \tag{39}$$

where

$$\Lambda_c^2 = \frac{\text{Continuous power contained outside the band } (-W, W)}{\text{Total power contained in the continuous part}}. \tag{40}$$

Note that $\Lambda_c^2 \neq \Delta^2$ or Δ_c^2, but

$$\frac{\Lambda_c^2}{\Delta_c^2} = \frac{\text{Total power in } \mathbf{P}_v(f)}{\text{Total power in } \mathbf{P}_{vc}(f)} \geqq 1. \tag{41}$$

Now Λ_c^2 can be made equal to $\Lambda_{\min}^2(WT)$ by choosing

$$x(t) = k\psi_0(t - T/2, d), \qquad d = \pi TW, \qquad T' = T, \tag{42}$$

where $\psi_0(t, d)$ is a prolate spheroidal wave function and k is a normalizing constant.† We choose k so that the total power E contained in the information-bearing part $\mathbf{P}_{vc}(f)$ [equivalently, the total energy contained in $x(t)$] is maximum. Since $\psi_0(t, d)$ is maximum at $t = 0$, E is maximized by choosing

$$g(t) = \begin{cases} \dfrac{2}{\pi} \operatorname{Sin}^{-1} \left\{ \dfrac{\psi_0(t - T/2, d)}{\psi_0(0, d)} \right\}, & 0 < t \leqq T,^{\ddagger} \\ 0, & \text{otherwise.} \end{cases} \tag{43}$$

For this value of $g(t)$,

$$E = \frac{\lambda_0}{T\psi_0^2(0, d)}. \tag{44}$$

For $x(t)$ in (42) and $g(t)$ in (43), the minimum out-of-band power ratio $\Lambda_{\min}^2(WT)$ can be attained, and

$$\Lambda_{\min}^2(WT) = 1 - \lambda_0. \tag{45}$$

For some values of d, the minimum out-of-band power ratio $\Lambda_{\min}^2(WT)$ and the maximum power contained in the continuous part are listed in Table I.§ The rest of the power in the PSK signal is contained in $\mathbf{P}_{vl}(f)$ or the discrete lines. For binary PSK, it follows from Sec. VI and eqs. (39) and (42) that $[\Lambda_c^2]_{\min}$ is given in Fig. 9.

---

* Since $|x(t)| \leqq 1$, note that Ω is a proper subset of $\mathcal{L}^2_\infty$.
† Our letter d in $\psi_0(t, d)$ corresponds to the letter c used in Refs. 8, 9, and 18.
‡ $\theta = \operatorname{Sin}^{-1}(x)$ denotes the principal value of the inverse sine, $-\pi/2 \leqq \theta \leqq \pi/2$.
§ We chose the values of d given in Table I so that we can make use of the results given in Refs. 8, 9, and 18.

Table I — Minimum out-of-band power ratio of binary PSK

$d = \pi TW$	WT	Minimum Out-of-Band Power Ratio $\Lambda^2_{\min}(WT)$	Maximum Normalized Power Contained in the Continuous Part of $\mathbf{P}_v(f)$
0.5	0.1592	0.6903	0.9730
1.0	0.3183	0.4274	0.9015
2.0	0.6366	0.1194	0.7122
4.0	1.2732	0.00411	0.4736

For $d = 0.5$, 1.0, 2.0, and 4.0, we plot the optimum $g(t)$ from (43) in Fig. 10. For $g(t)$ in (43) and Fig. 10, we plot the spectral density $\mathbf{P}_{v_c}(f)$ of binary PSK in Fig. 11.

From (11), $\Delta^2 = \Delta_l^2 + \Delta_c^2$, and since one usually specifies the total out-of-band power ratio, we list in Table II Δ_l^2, Δ_c^2, and Δ^2 for $g(t)$ in (43) and WT in Table I. Also for $g(t)$ in (43), we plot the *total* out-of-band power in Fig. 12. Comparing Figs. 1, 2, and 12, note that the total out-of-band power for the optimum pulse is very close to that for the rectangular pulse for $0 \leqq 2WT \leqq 1$. In the neighborhood of

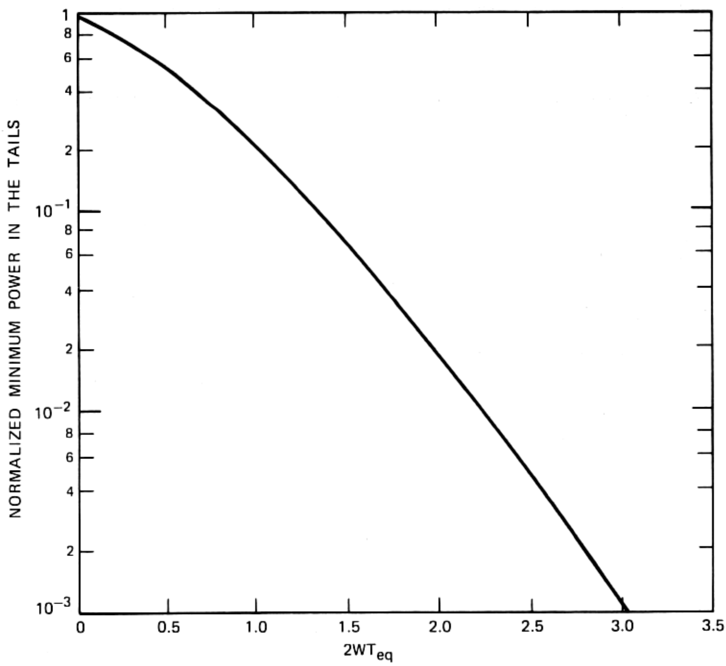

Fig. 9—Lower bound on the fractional energy contained outside the band $[-W, W]$ when the pulse $f(t)$ is of duration T_{eq}.

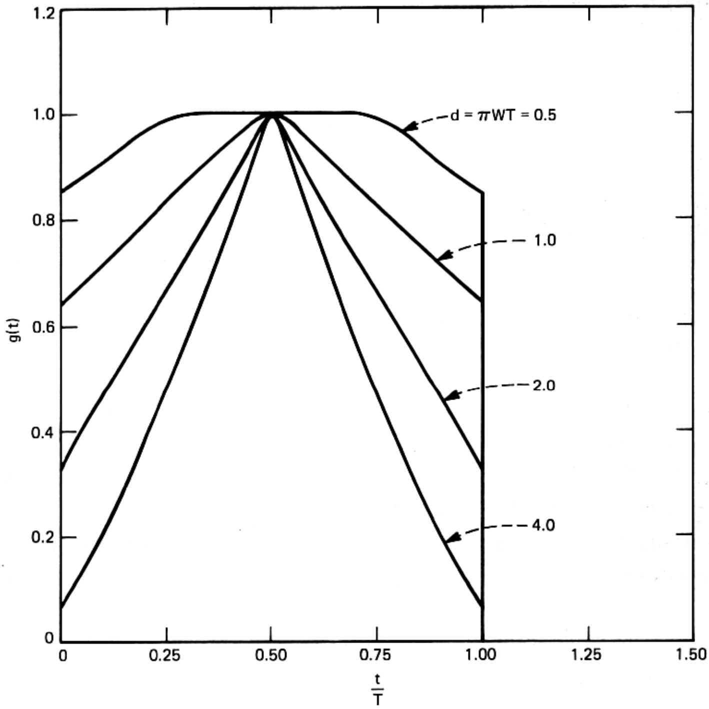

Fig. 10—Phase modulation pulse $g(t)$ for binary PSK for optimum continuous spectral occupancy.

$2WT = 0$, the total out-of-band power with the optimum pulse is greater than that with cosine, raised-cosine, triangular, or trapezoidal pulse. This is because the optimum pulse minimizes the fractional out-of-band *continuous* power and not the total power. For $g(t)$ in (43), it must be noted that the smaller the out-of-band continuous power ratio, the smaller the maximum amount of power contained in the continuous part. The rest of the power is contained in the discrete lines.*

One must note that, in general,

$$\Delta^2 \neq \Lambda^2_{\min}(WT) \tag{46}$$

the total out-of-band power ratio (the total out-of-band power divided

* The total out-of-band power with optimum pulse increases as a function of $2WT$ if we use the pulse in (43) and if $2WT > 2.5$. This is because an increasingly large amount of power is contained in the discrete lines and the total out-of-band discrete power very much dominates the out-of-band continuous power. By choosing the pulse which is optimum for $2WT \leqq 2.5$, we can make the total out-of-band power a monotone-decreasing function of $2WT$.

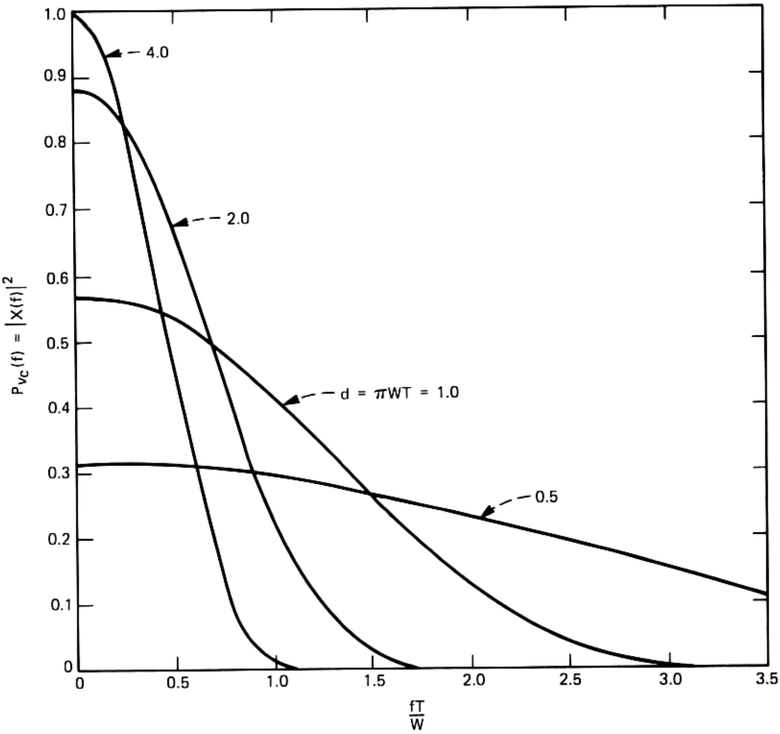

Fig. 11—Continuous spectral density $\mathbf{P}_{v_c}(f)$ of binary PSK for optimum continuous spectral occupancy.

by total power) is not equal to the out-of-band continuous power (the out-of-band continuous power divided by power contained in the continuous part). Also note that we have obtained a lower bound on $\Lambda^2_{\min}(WT)$ and not on Δ^2. Since any time function $y(t)$ containing discrete lines does not belong to $\mathcal{L}^2_\infty$, analysis given in Refs. 8 and 9 does not enable the optimization of Δ^2.

Our efforts to find a lower bound on the *total* band occupancy of a BPSK signal have not been successful so far, and it is suggested as an interesting problem for the reader.

So that we may compare the spectral occupancy of binary PSK with several different modulation pulses for $\Delta^2 = 0.1$, 0.01, and 0.001, we list in Table III the values of $2WT$.

Let us now consider a QPSK signal. From (22) one can show that no single function $x(t)$ can be found such that its energy density spectrum $|X(f)|^2$ is equal to $\mathbf{P}_{v_c}(f)$. If $2WT$ is large so that a small amount of total power is contained in the tails, we feel that the total out-of-band

Table II — Total out-of-band power ratio for binary PSK with $g(t)$ given by (43)

d	WT	Normalized Power Contained in the Continuous Part $\mathbf{P}_{vc}(f)$	Normalized Power Contained in the Discrete Part $\mathbf{P}_{vl}(f)$	Minimum Out-of-Band Continuous Power Δ_c^2	Out-of-Band Discrete Power Δ_l^2	Total Out-of-Band Power Ratio Δ^2	Normalized Power in the Lines at Frequency n/T from the Carrier	
0.5	0.1592	0.9730	0.0269	0.6717	0.00668	0.6784	$n = 0$	0.02024
1.0	0.3183	0.9015	0.0985	0.3853	0.02368	0.4090	$n = 0$	0.07483
2.0	0.6366	0.7122	0.2878	0.08506	0.06258	0.1476	$n = 0$	0.2252
4.0	1.2732	0.4736	0.5264	0.001943	0.00721	0.009153	$n = 0$	0.4364
							$n = \pm 1$	0.04139

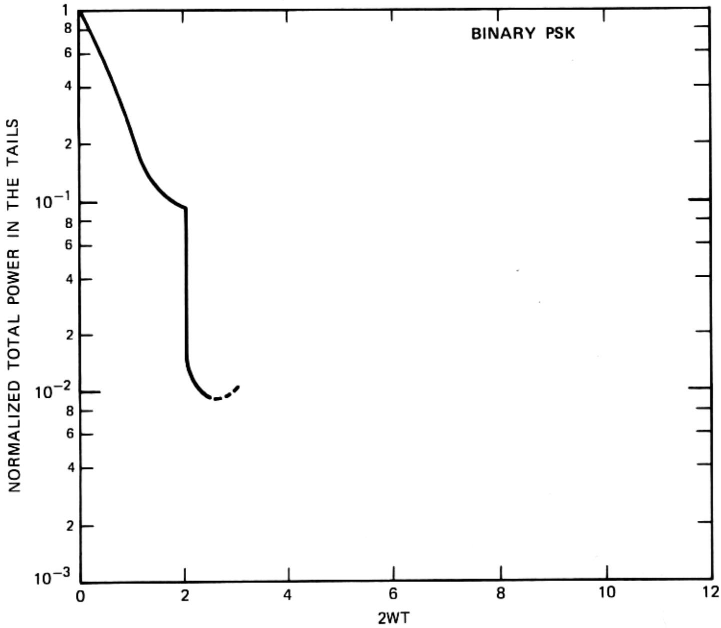

Fig. 12—Normalized total power contained outside the band $[-W, W]$ for $g(t)$ in (43). Observe that the total out-of-band power for $g(t)$ in (43) increases (see the dashed portion of the figure) as a function of $2WT$ for $2WT > 2.5$. This is because the total out-of-band discrete power, which is not optimized, very much dominates the out-of-band continuous power. Note that $g(t)$ in (43) only minimizes the fraction of the continuous power contained outside the band $[-W, W]$. For $2WT > 2.5$, by choosing $g(t)$ which is optimum for $2WT \leqq 2.5$, we can make the total out-of-band power decrease as a function of $2WT$.

power for a QPSK signal is lower-bounded by the results given for a BPSK signal. The band occupancy of QPSK for $\Delta^2 = 0.1, 0.01$, and 0.001 for different modulation pulses is listed in Table IV.

We now derive a lower bound on the *total* band occupancy of an FM-PSK signal. In (29) and (30), $g(t) \in \mathcal{L}^2_\infty$ is assumed to be completely arbitrary.

By defining

$$R_{t_1} = j\,\frac{e^{j(\pi fT-\pi/4)} + e^{-j(\pi fT-\pi/4)}}{2}\,R_1, \tag{47}$$

$$R_{t_2} = j\,\frac{e^{j(\pi fT-\pi/4)} - e^{-j(\pi fT-\pi/4)}}{2}\,R_2, \tag{48}$$

we can show from (28) that

$$\mathbf{P}_v(f) = \frac{1}{T}\,|R_{t_1} - R_{t_2}|^2 = |X(f)|^2, \tag{49}$$

Table III — Values of out-of-band power ratio Δ^2 for binary PSK with different baseband modulation pulses

Pulse $g(t)$ $g(t) = 0, t \leqq 0, t > T$	Normalized Power Contained in $\mathbf{P}_{v_c}(f)$	Total Out-of-Band Power Ratio Δ^2		
		0.1	0.01	0.001
		$2WT$	$2WT$	$2WT$
Rectangular $g(t) = 1, 0 < t \leqq T$	1.000	1.807	19.295	
Trapezoidal $g\left(t+\frac{T}{2}\right) = \begin{cases} 1, & 0 < \lvert t\rvert \leqq \frac{T}{4} \\ 2\left(1 - \frac{2\lvert t\rvert}{T}\right), & \frac{T}{4} \leqq \lvert t\rvert \leqq \frac{T}{2} \end{cases}$	0.750	2.000	4.000	8.000
Triangular $g\left(t+\frac{T}{2}\right) = 1 - \frac{2\lvert t\rvert}{T}$ $0 < \lvert t\rvert \leqq \frac{T}{2}$	0.500	2.000	3.283	6.000
Cosinusoidal $g\left(t+\frac{T}{2}\right) = \cos\frac{\pi t}{T},$ $0 < \lvert t\rvert \leqq \frac{T}{2}$	0.652	2.000	3.744	6.246
Raised-Cosinusoidal $g(t) = \frac{1}{2}\left(1 - \cos\frac{2\pi t}{T}\right),$ $0 < t \leqq T$	0.500	2.000	2.958	4.904

Table IV — Values of out-of-band power ratio Δ^2 for quaternary PSK with different baseband modulation pulses. Expressions for $g(t)$ are given in Table III

Pulse $g(t)$	Normalized Power Contained in $\mathbf{P}_{v_c}(f)$	Total Out-of-Band Power Ratio Δ^2		
		0.1	0.01	0.001
		$2WT$	$2WT$	$2WT$
Rectangular	1.000	1.807	19.295	
Trapezoidal	0.769	2.000	5.389	8.672
Triangular	0.538	2.000	3.651	6.274
Cosinusoidal	0.682	2.000	3.839	6.270
Raised-Cosinusoidal	0.526	2.000	4.000	5.491

where $X(f)$ is the Fourier transform of $x(t)$ and

$$x(t) = \begin{cases} \frac{1}{\sqrt{T}} \sin\left\{2\pi f_d \int_0^t g(\mu)d\mu\right\}, & 0 < t \leqq T, \\ \frac{1}{\sqrt{T}} \cos\left\{2\pi f_d \int_0^{t-T} g(\mu)d\mu\right\}, & T \leqq t \leqq 2T, \\ 0, & \text{otherwise.} \end{cases} \tag{50}$$

Since $x(t)$ may be nonzero only over an interval $(0, 2T)$ it follows that the minimum out-of-band power ratio Δ^2 of a binary FM-PSK is lower-bounded by*

$$\Delta^2 \geqq \Lambda^2_{\min}(WT_{\text{eq}}), \qquad T_{\text{eq}} = 2T, \tag{51}$$

where $\Lambda^2_{\min}$ is defined by (45). For $2WT \gg 1$, one can show[19] that

$$\Delta^2 \geqq \Lambda^2_{\min}(2WT) \sim 4\pi\sqrt{2WT}\left(1 - \frac{3}{64\pi WT}\right) \exp(-4\pi WT). \tag{52}$$

Note that $x(t)$ is not completely arbitrary over the interval $(0, 2T)$. From (50) one can show that if

$$x(t) = x_T(t), \qquad 0 < t \leqq T, \tag{53}$$

then

$$x(t) = \sqrt{\frac{1}{T} - x_T^2(t - T)}, \qquad T \leqq t \leqq 2T. \tag{54}$$

Equations (25) and (50) also yield

$$x(0) = 0 \tag{55}$$

and

$$x(T) = \frac{1}{\sqrt{T}}. \tag{56}$$

When $x(t) \in \mathfrak{L}^2_\infty$ is completely arbitrary, the lower bound in (51) is attained when

$$x(t) = k\Psi_0(t - T, d), \qquad d = 2\pi TW, \qquad T' = 2T, \tag{57}$$

where $\Psi_0(t, d)$ is defined in Section VI. Any function other than (57) has a larger out-of-band power ratio. Since $x(t)$ in (57) does not satisfy (53) to (56), it follows that the bound in (51) is strictly a lower bound and is not attainable.†

* Note that there is no discrete power contained in an FM-PSK signal.

† The derivation of an attainable lower bound is extremely complicated and will not be attempted here. Also, Table V shows that rectangular signaling gives a bandwidth occupancy which is very close to the lower bound when $\Delta^2 \approx 0.01$, the region of interest.

Table V — Values of the lower bound on $2WT$ and of bandwidth occupancy for binary FM-PSK with rectangular and raised-cosine signaling

Pulse $g(t)$ $g(t) = 0,\ t \leqq 0,\ t > T$	Rectangular $g(t) = 1$, $0 < t \leqq T$	Raised-Cosinusoidal $g(t) = \frac{1}{2}\left(1 - \cos\frac{2\pi t}{T}\right)$, $0 < t \leqq T$	Lower Bound on $2WT$
(Peak-to-Peak Frequency Deviation) $\times T$	0.5	1.0	
Out-of-Band Power Ratio Δ^2	(Bandwidth Occupancy $2W$) $\times T$		
0.1	0.773	0.930	0.675
0.01	1.170	2.200	1.117
0.001	2.578	2.874	1.517

The values of the lower bound on $2WT$ and of band occupancy of binary FM-PSK for $\Delta^2 = 0.1$, 0.01, and 0.001 with rectangular and raised-cosine signaling are listed in Table V. The lower bound on Δ^2 given by (51) is also plotted in Fig. 8. Note that the lower bound is very close to Δ^2 with rectangular signaling for $1 \leqq \Delta^2 \leqq 0.01$.

Note that the bandwidth occupancy of binary FM-PSK with rectangular signaling is smaller than that with raised-cosine signaling if $\Delta^2 \geqq 0.001$.* Note also that the peak-to-peak frequency deviation with raised-cosine signaling is larger than that with rectangular signaling. The phase deviation in one signaling interval is always $\pm\pi/2$.

VIII. CONCLUSIONS

For binary and quaternary PSK systems, the band occupancy results presented here can be combined with the results given in Ref. 7 so that channel bandwidth and channel spacing can be chosen to produce minimum distortion transmission and to satisfy any specified power occupancy criterion. The band occupancy of PSK with overlapping baseband pulses is known to be narrower,[10] but we have not considered such signals in this paper.

The 99-percent power occupancy bandwidth of an FM-PSK signal with rectangular signaling is shown to be only 4.7 percent higher than the lower bound. The channel spacing requirements of FM-PSK, from

* The tails of the FM-PSK spectra with raised-cosine signaling go as $\sim 1/f^8$, with rectangular signaling as $\sim 1/f^4$. Hence, the bandwidth occupancy with raised-cosine signaling becomes smaller than that with rectangular signaling for small enough $\Delta^2 (\Delta^2 < 7.5 \times 10^{-4})$.

the point of view of distortion produced by adjacent channel interference, will be treated in subsequent work.

An attempt is also being made to derive a lower bound on the band occupancy if the total power in the continuous part of a BPSK signal is a specified fraction of the total RF power.

IX. ACKNOWLEDGMENTS

Discussions with Larry J. Greenstein, John J. Kenny, and Harrison E. Rowe are gratefully acknowledged.

REFERENCES

1. L. C. Tillotson, C. L. Ruthroff, and V. K. Prabhu, "Efficient Use of the Radio Spectrum and Bandwidth Expansion," Proc. IEEE, *61* (April 1973), pp. 445–452.
2. C. K. H. Tsao and E. M. Perdue, "RF Wideband Data Terminal," Raytheon Company Technical Report, Wayland, Mass., February 1974.
3. H. E. Rowe, *Signals and Noise in Communication Systems,* New York: Van Nostrand, 1965, pp. 57–202.
4. L. Lundquist, "Channel Spacing and Necessary Bandwidth in FDM-FM Systems," B.S.T.J., *50,* No. 3 (March 1971), pp. 869–880.
5. A. Anuff and M. L. Liou, "A Note on Necessary Bandwidth in FM Systems," Proc. IEEE, *59,* No. 10 (October 1971), pp. 1522–1523.
6. V. M. Ray, *Interpreting FCC Broadcast Rules and Regulations,* Blue Ridge Summit, Pa.: TAB Books, 1966.
7. V. K. Prabhu, "Bandwidth Occupancy in PSK Systems," IEEE Trans. Comm., *COM-25* (April 1976), pp. 456–462.
8. D. Slepian and H. O. Pollak, "Prolate Spheroidal Wave Functions, Fourier Analysis and Uncertainty—I," B.S.T.J., *40,* No. 1 (January 1961), pp. 43–63.
9. H. J. Landau and H. O. Pollak, "Prolate Spheroidal Wave Functions, Fourier Analysis and Uncertainty—II," B.S.T.J., *40,* No. 1 (January 1961), pp. 65–84.
10. V. K. Prabhu and H. E. Rowe, "Spectra of Digital Phase Modulation by Matrix Methods," B.S.T.J., *53,* No. 5 (May–June 1974), pp. 899–935.
11. T. T. Tjhung, "Band Occupancy of Digital FM Signals," IEEE Trans. Comm., *COM-12* (December 1964), p. 211.
12. R. deBuda, "Coherent Demodulation of Frequency-Shift Keying with Low Deviation Ratio," IEEE Trans. Comm., *COM-20* (June 1972), pp. 429–435.
13. H. E. Rowe and V. K. Prabhu, "Power Spectrum of a Digital FM Signal," B.S.T.J., *54,* No. 6 (July–August 1975), pp. 1095–1125.
14. W. A. Sullivan, "High-Capacity Microwave System for Digital Data Transmission," IEEE Trans. Comm., *COM-20* (June 1972), pp. 466–470.
15. D. M. Brady, "FM-CPSK: Narrowband Digital FM with Coherent Phase Detection," Proc. Int. Conf. on Communications, Philadelphia, Pa., June 1972, pp. 44.12–44.16.
16. D. M. Brady, "Spectra for FM-DCPSK Modulation," unpublished work.
17. W. Hilberg and P. G. Rothe, "The General Uncertainty Relations for Real Signals in Communication Theory," Information and Control, *18* (1971), pp. 103–125.
18. C. Flammer, *Spheroidal Wave Functions,* Stanford, Calif.: Stanford University Press, 1957.
19. D. Slepian and Mrs. E. Sonnenblick, "Eigenvalues Associated with Prolate Spheroidal Wave Functions of Zero Order," B.S.T.J., *44,* No. 8 (October 1965), pp. 1745–1759.